An Energy Balance Model Based on Potential Vorticity Homogenization

DANIEL B. KIRK-DAVIDOFF

Harvard University, Cambridge, Massachusetts

RICHARD S. LINDZEN

Massachusetts Institute of Technology, Cambridge, Massachusetts

(Manuscript received 6 July 1998, in final form 19 February 1999)

ABSTRACT

It has long been suggested that the extratropical eddies originating in baroclinic instability act to neutralize the atmosphere with respect to baroclinic instability. These studies focused on the Charney–Stern condition for stability, and since the implication of this condition was the elimination of meridional temperature gradients at the surface, contrary to observations, there appeared little possibility that the hypothesis was correct.

However, Lindzen found that potential vorticity (PV) mixing along isentropic surfaces accompanied by elevated tropopause height and/or reduced jet width could also lead to baroclinic neutralization. Since it is not obvious what implications such a neutral state would have for meridional structure of wind and especially temperature, the authors examine, as a first step, in this paper the implications of an assumed fixed PV gradient in the extratropical troposphere.

It is shown that this assumption, combined with an assumption of a moist adiabatic temperature structure in the Tropics, a constraint on surface static stability, and overall radiative equilibrium, suffices to constrain a model earth's zonal mean climate. Comparison of the model climate with the observed climate, and variation of certain of the model's assumptions to resolve differences, allow the authors to consider the role of deep convection in the climate of the midlatitudes, to investigate the connection between surface turbulent heat fluxes and meridional energy fluxes carried by baroclinic eddies, and to deduce the role of the stratosphere's overturning circulation in determining the height of the tropopause.

1. Introduction

Several theories have been advanced to describe the interaction of atmospheric eddies with climate. Sellers (1969), in designing a one-dimensional energy balance climate model, assumed that the eddies behaved as a diffusive term acting on the meridional temperature distribution. The eddy diffusion term could then be coupled with a radiation parameterization to determine the earth's zonal mean climate. Stone (1978) and Lindzen and Farrell (1980) theorized that eddies act to keep the atmosphere marginally stable to their own growth by eliminating the change in sign in potential vorticity (PV) gradient at the earth's surface, which is a necessary condition for baroclinic instability (Charney and Stern 1962). In Stone's approach, this translated directly into a neutral temperature gradient that could be approached but not much exceeded, while Lindzen and Farrell used the heat fluxes implicit in neutralization to adjust the temperature gradient to an equilibrium value. General circulation models (GCMs) make the implicit assumption that the energy-carrying eddies must be explicitly resolved in order to be correctly modeled.

Each of these approaches has disadvantages. Modeling eddies as a diffusive influence on surface temperature begs the question, what sets the value of the diffusivity? We know from the geological record that climate states (e.g., the Eocene, 50 Myr) have existed in which the earth's mean meridional temperature gradient was much smaller than it currently is. Such climates require larger meridional energy fluxes (Rind and Chandler 1991) to support warm polar temperatures; clearly the relationship between heat fluxes and temperature gradient was different in the Eocene than at present. Theories of eddy heat fluxes that require them to remove the change in sign of the PV gradient are confronted with the fact that in the real atmosphere, such a change in sign is always present. This is because the negative meridional temperature gradient at the surface implies a negative PV gradient there (Bretherton 1966), while the increasing stability along isentropes entering the stratosphere guarantees a positive PV gradient in the vicinity of the tropopause. Finally, because GCMs at-

Corresponding author address: Dr. Daniel B. Kirk-Davidoff, Department of Chemistry and Chemical Biology, Harvard University, 12 Oxford St., Cambridge, MA 02138.
E-mail: davidoff@huarp.harvard.edu

tempt to include all physics relevant to climate, it can be difficult to identify the processes most responsible for a certain effect. A possibly better measure of our understanding of a physical process is our ability to predict the behavior of interest using a model that contains only the mechanisms we think relevant.

In this paper we discuss a new approach toward the connection of baroclinic instability theory with climate dynamics. We will consider the hypothesis that the primary climatological role of atmospheric eddies is to mix PV in the free troposphere, thus connecting the tropospheric PV to that of the boundary layer. Because the distribution of PV determines the slopes of isentropes with respect to one another, the degree of PV mixing is a strong constraint on the temperature distribution of the troposphere, which in turn, through radiative interactions, has a strong influence on the surface temperature structure.

This approach is motivated by the work of Lindzen (1993), who showed that the troposphere could be made neutral to the linear growth of baroclinic disturbances if PV gradients were removed up to a certain height (dependent on the width of the subtropical jet), and who associated this height with the tropopause. In particular, Lindzen (1993) proposed that the height of the tropopause, H, should satisfy the equation: $H \leq r[(4/3)s^2 + r^2/L^2]^{-1/2} \times 2.3994 f/N$, where r is the earth's radius, f is the Coriolis parameter, N is the Brunt–Väisälä frequency, L is the half-width of the zonal mean jet, s is the zonal wavenumber, the factor of 4/3 derives from the assumed location of the jet at 30°, and the number 2.3994 arises from the solution for the shortwave cutoff of the Eady problem.

Numerical studies of Lindzen's (1993) hypothesis have had mixed results. Thuburn and Craig (1997) in a GCM study found that when f was reduced, there was an increase in the mean jet width, consistent with Lindzen's hypothesis. However, no such compensation was observed when perturbations in the surface temperature or ozone concentration led to changes in tropopause height. Nakamura (1998) has confirmed in experiments with a quasigeostrophic two-layer f-plane model that initially unstable flows can be neutralized when the flow evolves to a state where barotropic shear constrains the meridional extent of eddies, yielding neutralization via the shortwave cutoff. However, experiments on a β plane yielded neutralization via the elimination of PV gradients in the lower layer.

Sun and Lindzen (1994) demonstrated that the temperature structure of the midlatitude troposphere could be well approximated by assuming small PV gradients and by using the resulting relationship among the slopes of isentropes to integrate the tropospheric temperatures from boundaries at the earth's surface and at the poleward edge of the Tropics. More detailed, seasonal analysis of the zonal mean potential vorticity distribution shows that true homogenization of PV along extratropical isentropes is confined to the region between 600 and 800 mb, as shown in Fig. 1.

The observation that homogenization is confined to this relatively narrow region throws doubt on the validity of the assumption that PV values at the surface can be efficiently transmitted to the interior. However, the observations shown in Fig. 1 do show that the seasonal variations of PV gradients are relatively small. Further, modeling studies by Solomon (1998) indicate that the limited region of well-mixed PV contributes significantly to the stabilization of the mean flow to the growth of baroclinic eddies. Thus, rather than focus on the precise nature or degree of homogenization or of baroclinic stabilization, we wish, in this paper, to show how, due to the strong dependence of PV on static stability, any fixed zonal mean PV distribution can be used to predict the zonal mean temperature structure, given sufficient boundary information. Future studies may provide for a more detailed and mechanistic approach to PV mixing.

The connection between PV and temperature makes possible an extension of the one-dimensional convective adjustment model to two dimensions. In a convective adjustment model, one assumes that cumulus convection acts to maintain a marginally conditionally stable vertical distribution of saturation moist entropy, or alternatively, an ad hoc temperature distribution intended to reproduce observations. Here we assume that PV is partially homogenized along isentropes by the action of baroclinic eddies. This assumption implies that large-scale turbulent mixing in the troposphere mixes PV between the planetary boundary layer and the tropospheric interior in such a way that the gradient of PV between these regions remains constant from one season to the next. We have no strong theoretical justification for this assumption, but we note observational evidence of small seasonal variations in the zonal mean PV distribution. As with the moist adjustment model, we can couple a procedure for determining the atmosphere's temperature with a radiative code in order to define a climate that is in overall radiative balance and meets some dynamical criterion, in this case a prescribed gradient of PV. As we will show, several additional assumptions are necessary to define that climate uniquely. Variation of these assumptions allows us to test hypotheses about the origins and roles of several features of the observed climate and climate history, such as the meridional variation of the tropopause height, the temperature structure of polar regions, and the poleward amplification of climate change.

The most problematic of these assumptions have to do with the specification of the surface lapse rate. If it is specified arbitrarily, then the height of the tropopause must be allowed to be set internally, in order to preserve temperature continuity between the troposphere and the stratosphere. If, on the other hand, the height of the tropopause is set arbitrarily to satisfy a theoretical baroclinic neutrality criterion, then the surface lapse rate

must be adjusted to assure continuity at the tropopause, and the resulting climate becomes highly sensitive to conditions in the stratosphere. Other options and compromises will be discussed. Each of the possible closures has different implications for the meridional response of the model climate to perturbations of its radiative parameters.

2. Model description

In this section, we will explore the extent to which a requirement of a fixed PV gradient constrains the calculated climate. We will show that fixing the PV gradient along isentropes results in an easily integrable differential equation in the gradient of potential temperature with pressure, $\partial\theta/\partial p$. Thus, if $\partial\theta/\partial p$ is known at some location on every isentrope, it can be predicted everywhere. If the temperature at the surface is specified, $\partial\theta/\partial p$ can be integrated to yield θ, and thus temperature, at every pressure and latitude.

This information can, with additional assumptions about the distribution of water vapor and cloud, be used to predict radiative fluxes. The surface temperature can then be adjusted so that the energy budgets of the surface and of the model as a whole are balanced. Differences between the resulting model climate and the observed climate will point to flaws or omissions in our assumptions; by modifying those assumptions, we can gain insight into the physical processes potentially responsible for the observed climate.

The surface temperature is adjusted by integrating the thermodynamic equation for the earth's surface:

$$\rho D C_l \frac{1}{\Delta A}\frac{\partial T_s(\phi)}{\partial t} = F_{\mathrm{IR}}(\phi) + F_{\mathrm{SO}}(\phi) + F_{\mathrm{SH}}(\phi) + F_{\mathrm{LH}}(\phi) + F_O(\phi), \quad (1)$$

where ρ is the density of liquid water; $D = 50$ m is the depth of the ocean mixed layer taken to constitute the surface of the model; C_l is the heat capacity of liquid water; T_s is the temperature of the mixed layer; t is time; ϕ is latitude; F denotes a downward directed energy flux per unit area; the subscripts IR, SO, SH, and LH denote fluxes of infrared radiation, solar radiation, sensible heat and latent heat, respectively; while F_O represents the meridional flux convergence per unit area of the poleward oceanic heat flux. To construct an energy balance model, it is necessary to relate the various fluxes to the surface temperature.

a. Extratropical temperatures

Calculation of the radiative fluxes requires an estimate of the atmosphere's temperature and its cloud and trace gas content. Figure 2 shows how temperatures are calculated in various regions represented in the model. We begin by using our assumption of fixed PV to calculate the atmosphere's temperature, given the temperature at the surface. PV in isentropic coordinates is

$$P = -g(f + \zeta)\left(\frac{\partial p}{\partial \theta}\right)^{-1}, \quad (2)$$

where P is the PV, g is the acceleration of gravity, f is the Coriolis parameter, ζ is the relative vorticity, p is the pressure, and θ is the potential temperature. Differentiating with respect to y gives

$$\frac{\partial P}{\partial y} = -g\frac{\partial(f+\zeta)}{\partial y}\left(\frac{\partial p}{\partial \theta}\right)^{-1} + g(f+\zeta)\left(\frac{\partial p}{\partial \theta}\right)^{-2}\frac{\partial^2 p}{\partial y \partial \theta}. \quad (3)$$

The term $-g\beta(\partial p/\partial\theta)^{-1}$, where $\beta = \partial f/\partial y$, will be referred to hereinafter as the β contribution to the PV gradient. We will require the PV gradient to be equal to a given fraction, $\gamma(p)$ of this β contribution. In this paper, we set $\gamma(p)$ equal to a constant everywhere; in work in progress we consider the sensitivity of the model to the vertical structure of γ. The observed distribution of γ is shown in Fig. 3.

Observations of temperature and wind show that for the zonal mean circulation, ζ, the relative vorticity, is generally much smaller than f, the planetary vorticity. Sun and Lindzen (1994) showed that neglecting the relative vorticity in the derivation of temperature from a fixed PV distribution introduced only small errors. Thus, in the following calculations and modeling, ζ will be ignored. Setting $\zeta = 0$, and substituting $\partial P/\partial y = -\gamma g(\partial f/\partial y)(\partial p/\partial\theta)^{-1}$ in Eq. (3) yields

$$(1-\gamma)\frac{\partial f}{\partial y}\left(\frac{\partial p}{\partial \theta}\right) = f\frac{\partial^2 p}{\partial y \partial \theta} \quad (4)$$

$$\int_{y_0}^{y}(1-\gamma)\frac{\partial}{\partial y}\ln f\, dy = \int_{y_0}^{y}\frac{\partial}{\partial y}\ln\left(\frac{\partial p}{\partial\theta}\right) dy. \quad (5)$$

Integration yields

$$\frac{\partial p}{\partial \theta} = \left.\frac{\partial p}{\partial \theta}\right|_{y_0}\left(\frac{\sin\phi}{\sin\phi_0}\right)^{(1-\gamma)}, \quad (6)$$

where ϕ is latitude, $y = a\phi$, and a is the earth's radius. Note that when $\gamma = 1$, Eq. (6) requires that the lapse rate of θ with p be constant along isentropes, while $\gamma < 1$ implies that the lapse rate becomes less stable as latitude increases, and $\gamma > 1$ implies that the lapse rate becomes more stable as latitude increases.

This relationship can be integrated over potential temperature to obtain the pressure of each isentrope for all latitudes outside the Tropics:

$$p(\phi, \theta) = \int_{\theta_s}^{\theta}\left.\frac{\partial p}{\partial \hat{\theta}}\right|_{\phi_t}\left(\frac{\sin\phi}{\sin\phi_t}\right)^{(1-\gamma)} d\hat{\theta}, \quad (7)$$

where ϕ_t is the latitude at which θ intersects either the lower boundary or the latitude at the edge of the Tropics, which we fixed at 20° latitude in each hemisphere for

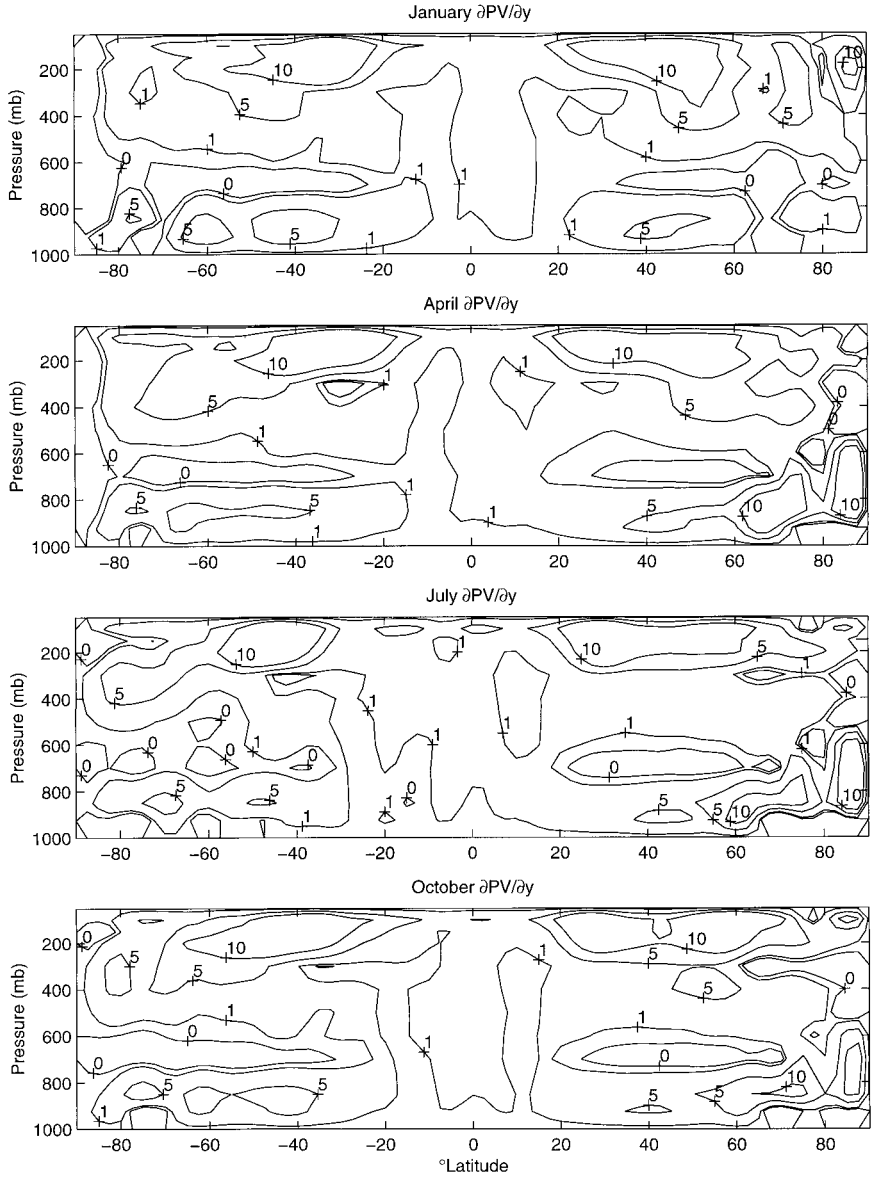

FIG. 1. Poleward meridional gradient of PV $[-g(f + \zeta)(\partial p/\partial\theta)^{-1}]$ on isentropes, calculated from zonal mean θ, for Jan, Apr, Jul, and Oct means, 1982–94. Contours are labeled in multiples of 10^{-13}m s^{-1} K kg^{-1}. Data from the NCEP–NCAR reanalysis project (Kalnay et al. 1996).

the purposes of the current paper. Boundary conditions are continuity in potential temperature and its pressure derivative along the vertical boundary of the Tropics and along a fixed surface pressure at the horizontal boundary near the model earth's surface. To satisfy the boundary conditions, we need to know θ and $\partial\theta/\partial p$ along the model-free troposphere's lower boundary outside of the Tropics, θ and $\partial\theta/\partial p$ along the vertical boundary between the Tropics and the extratropics, and the location of that boundary (ϕ_t). A sample θ distribution is shown in Fig. 4.

In the real atmosphere, a combination of turbulent fluxes driven by surface heating, and fluxes driven by free tropospheric motions must establish the mean lapse rate at the earth's surface. Here we consider two ways of specifying this boundary condition. One possibility is to simply assume that $\partial p/\partial\theta|_{y_0}$ along the surface has some fixed functional dependence on y. This allows us to test the sensitivity of the model to changes in the assumed dependence on y.

Alternatively, the height of the tropopause may be specified, as suggested by Lindzen (1993), and the surface static stability adjusted so that temperature is continuous across the tropopause. However, there are problems with this approach. First, Lindzen's (1993) specification of the tropopause height is one-dimensional:

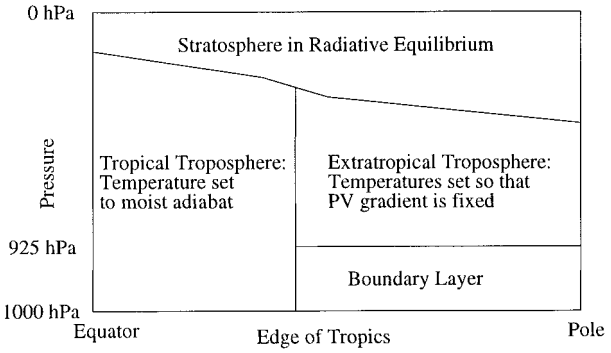

FIG. 2. Schematic of model structure.

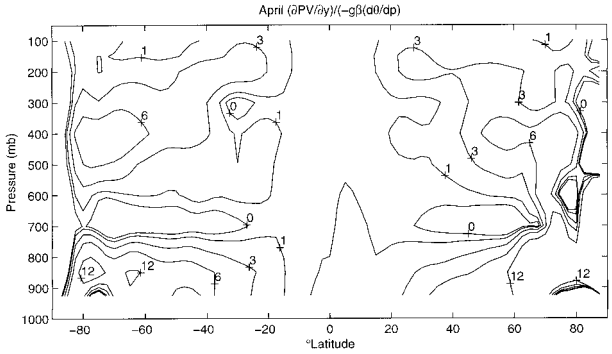

FIG. 3. Poleward meridional gradient of PV $[-g(f + \zeta)(\partial p/\partial\theta)^{-1}]$ on isentropes, calculated from zonal mean θ, divided by the β contribution to PV $[-g\beta(\partial p/\partial\theta)^{-1}]$, for average Apr 1982–94. Contours are labeled in multiples of the β contribution. Data from the NCEP–NCAR reanalysis project (Kalnay et al. 1996).

there is no way to predict the dependence of tropopause height on latitude. Even if there were, in this model the influence of surface static stability on tropopause height is sufficiently weak that it is not possible to guarantee temperature continuity at all latitudes if the height of the tropopause is fixed arbitrarily at all latitudes. Second, it is unclear whether the height of the tropopause or the width of the jet, should be adjusted, while Solomon's (1998) results show that total homogenization is unnecessary for neutralization and suggest that neutralization through redistribution of PV gradients is possible, even for a fixed tropopause height. Finally, specifying the tropopause height and adjusting the surface lapse rate to give continuity in temperature at the tropopause result in very high sensitivity of the equilibrium surface temperature to conditions in the stratosphere, since the equilibrium surface temperature depends very strongly on the surface static stability, but the temperature high in the troposphere depends fairly weakly on surface static stability.

A third closure that ties the surface temperature less tightly to the stratosphere is also possible. In this case the potential temperature of the polar tropopause is fixed, rather than the height of the tropopause everywhere. Specifically, the isentrope that intersects the top of the boundary layer at the boundary between the Tropics and extratropics is required to intersect the tropopause at the Pole, and the surface static stability is assumed to increase poleward with a slope that is adjusted until this requirement is met. Although we still lack a theoretical explanation for this choice, observations suggest that this coincidence is approximated throughout the seasonal cycle (Holton et al. 1995), and GCM modeling results show it to be a robust feature of the potential temperature distribution (T. Schneider 1998, personal communication).

b. Tropical temperatures

Assuming PV homogenization does not, of course, suffice to predict actual values of PV in the interior of the troposphere; we must first supply $\partial p/\partial\theta$ at the equatorward boundary of a PV-mixing region. In the Tropics, the overturning Hadley cell guarantees that temperature gradients will be small, while it can be argued that moist convection will maintain an approximately moist adiabatic lapse rate. This results in meridional PV gradients approximately equal to the β contribution. Although there is much debate over the degree to which moist convective adjustment obtains in the Tropics (Emanuel et al. 1994; Brown and Bretherton 1997), it is clear that the temperature in the high tropical troposphere, where convection detrains, must be connected to the surface temperature by a moist adiabat. The temperatures between may differ by a greater or lesser degree from that moist adiabat, but an assumption of moist neutrality will at least capture the layer mean static stability, and thus PV, at the poleward edge of the Tropics.

In our model, the temperature at each pressure level is set so that the pseudoequivalent potential temperature, θ_{ep} is equal to $\theta_{ep}(p_{surface})$. The pseudoequivalent potential temperature is a quantity that is conserved during the ascent of a parcel that conserves sensible heat but loses all water condensed from vapor during the ascent. It is defined as

$$\theta_{eq} = T\left(\frac{1000}{p}\right)^{0.2854(1-0.28r)} \times \exp\left[r(1 + 0.81r)\left(\frac{3.376}{T^*} - 2.54\right)\right]$$

(Emanuel 1994), where T is the temperature in kelvins; T^* is the temperature at which a surface parcel, lifted adiabatically, reaches saturation with respect to liquid water; p is the pressure in milibars; and r is the water vapor mixing ratio, in this case, that of a parcel lifted adiabatically from the surface.

The temperature profile corresponding to fixed θ_{ep} is calculated as follows. The water vapor mixing ratio is determined in the model by fixing the relative humidity at observed levels and then using the model temperature to calculate the saturation mixing ratio, r^*. Then r is

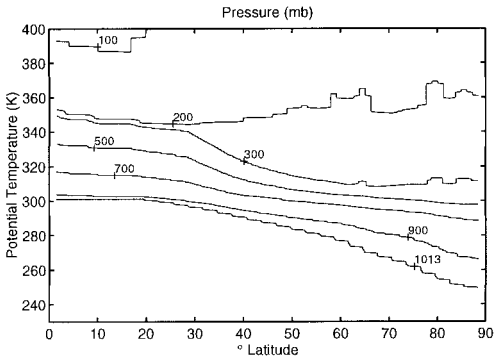

FIG. 4. Contours of pressure plotted on a θ–ϕ grid. Contours labeled in mb.

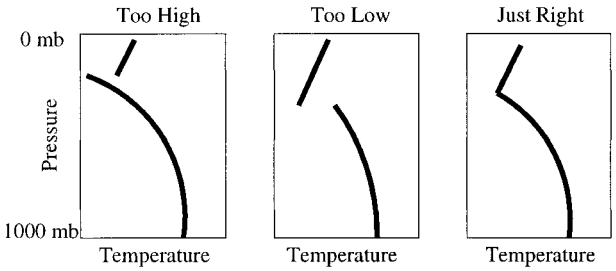

FIG. 5. Schematic depiction of tropopause height determination.

determined in this manner for the surface parcel. As the calculation of temperature proceeds upward in the atmosphere, r is held constant until $r^* = r$. Above this level, r is set equal to r^*. To find the temperature at a given level for which $\theta_{ep}(p) = \theta_{ep}(p_{surface})$, the temperature at the next lower level is chosen as an initial guess. First r and θ_{ep} are calculated for that temperature, pressure, and r^*; then T is increased by 0.01 K. The procedure is repeated until the temperature is found for which $\theta_{ep}(p) = \theta_{ep}(p_{surface})$.

c. Radiative parameters

We assume that surface albedo, trace gas concentrations, relative humidity, and cloud distributions are fixed. This is done to test the methodology and would be inappropriate for a predictive model. Fixing these quantities allows us to supply information that cannot be derived from our model to a radiative transfer model (Chou and Suarez 1994). The latter model can be given the temperature information derived above, and it is then able to return information about radiative heating rates and heat fluxes within the atmosphere and at the earth's surface.

The model of Chou and Suarez (1994) is a band model of thermal infrared radiation in the earth's atmosphere that uses a mixture of k-distribution and one- and two-parameter scaling in different spectral regions and pressure regimes to get optimal accuracy and speed. The code produces heating rates with an accuracy of 0.2 K day^{-1}, compared to line-by-line calculations. We use this model, along with the solar radiative transfer model of Chou (1986), to calculate net radiative heating rates and fluxes throughout the atmosphere.

The atmosphere is assumed to have a constant surface pressure of 1013.15 mb. The mixing ratio of carbon dioxide is set at 300 ppmv (a round number, corresponding to the carbon dioxide concentration of gas trapped in Antarctic ice around 1915; Neftel et al. 1994), and the ozone mixing ratio is set equal to a zonal mean climatology (Dütsch 1978). The concentration of water vapor, as a function of height and latitude, is determined by assuming a fixed distribution of relative humidity taken from Peixoto and Oort (1992). Similarly, for the purposes of calculating solar radiation, cloud height, depth, and fractional coverage are all supplied from the International Satellite Cloud Climatology Project (ISCCP) satellite cloud climatology (Drake 1993). For infrared radiative calculations, a simplified cloud distribution is used. Two cloud layers are set: one extending from 800 to 500 mb and the other from 400 to 200 mb, or the tropopause, whichever is lower. Cloud fraction for the lower cloud varies from 0.15 at the equator to 0.35 at the Poles, while the fractional coverage of the upper cloud ranges from 0.5 at the equator to 0.4 at the Poles. The two cloud layers are assumed to overlap randomly. These distributions were chosen to arrive at a climate in reasonable agreement with observations but are themselves in reasonable agreement with the ISCCP climatology. Annual mean solar forcing and annual mean climatologies of cloud properties, relative humidity, and surface albedo are used. Experiments with seasonally varying insolation, humidity, and albedo (but fixed PV gradient) show little difference in the annual mean climate. For simplicity, data from the Northern and Southern Hemispheres are averaged at opposite latitudes, so that insulation, humidity, and albedo have the same values at 50°N and 50°S.

d. Stratospheric temperatures

Figure 2 shows a stratosphere in radiative equilibrium above the model troposphere. If the rules used to determine atmospheric temperature in the Tropics and extratropics were applied up to the top of the atmosphere, temperatures there would be extremely low, in general less than 150 K at 25 mb. Such cold temperatures are never observed in the earth's atmosphere because high radiative heating rates due to the absorption of solar ultraviolet radiation imply much warmer radiative equilibrium temperatures. To account for this, the highest regions of the model are allowed to come into radiative equilibrium. As shown in Fig. 5, the height of the tropopause, above which the model is in radiative equilibrium, is determined through an iterative procedure. The tropopause height is first guessed, and the stratospheric temperatures allowed to come into radiative equilibrium. The temperature discontinuity between the

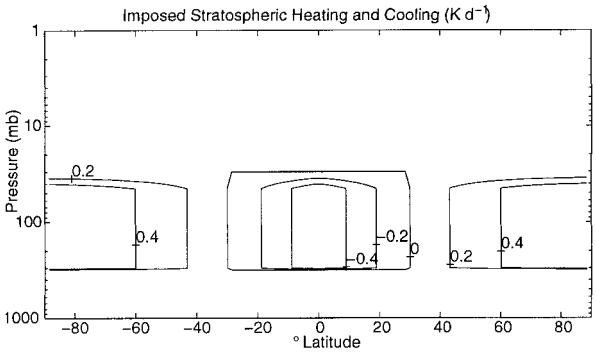

FIG. 6. Contours of heating rate (K day^{-1}) added to radiative heating to simulate overturning circulation of the stratosphere, plotted vs p and ϕ.

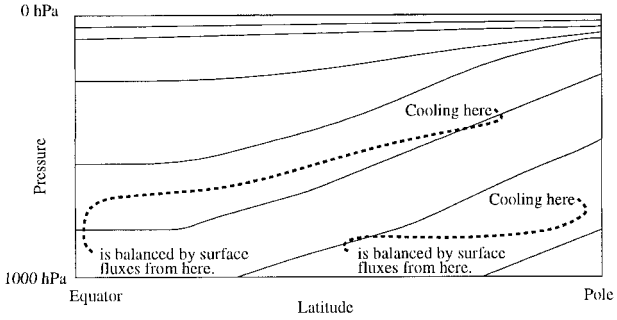

FIG. 7. Schematic of surface turbulent heat flux allocation. Solid lines are isentropes. Radiative heating on a given isentrope in the free troposphere is balanced by heat and moisture fluxes from the surface in the region where that isentrope intersects the surface. If the isentrope never intersects the surface, radiative cooling is balanced by convective heat fluxes that are initially assumed to take place in the Tropics only.

radiative equilibrium temperature calculated for the tropopause level and the temperature calculated for that level by the assumption of PV homogenization (or moist neutrality in the Tropics) can be calculated. The height of the tropopause can then be varied, and the process repeated until the temperature discontinuity is brought as close to zero as vertical resolution allows, generally less than 0.5 K for the resolution used here.

We include a representation of the observed stratospheric overturning circulation, by imposing dynamic cooling in the tropical stratosphere and warming in the polar stratosphere. Following Olaguer et al. (1992), heating and cooling are required to be balanced, so that they average to zero on pressure surfaces over the globe. The imposed dynamic heating and cooling profile is shown in Fig. 6. The cooling necessary to raise the tropical tropopause to observed heights is -0.5 K day^{-1}, and the warming needed to lower the polar tropopause to observed heights is 0.5 K day^{-1}, which are in reasonable agreement with radiative transfer calculations from observed temperatures and trace gas concentrations (Eluszkiewicz et al. 1997).

e. Turbulent heat fluxes

The assumptions made above are sufficient to allow the calculations of the terms $F_{\mathrm{IR}}(\phi)$ and $F_{\mathrm{SO}}(\phi)$ in Eq. (1). These two terms are not sufficient to calculate the surface temperature, however. First, assuming the turbulent fluxes $F_{\mathrm{SH}}(\phi)$ and $F_{\mathrm{LH}}(\phi)$ to be zero would result in the unrealistically warm surface temperatures characteristic of radiative equilibrium temperature structures (Goody 1995). Second, the assumptions made about the maintenance of moist adiabatic and PV-homogenized temperature structures imply an atmosphere which is not, in general, in radiative equilibrium, in either a point-by-point or a globally integrated sense. The imbalance must be made up by turbulent fluxes of heat from the surface. Additional assumptions are required to guide the allocation of these fluxes along the model surface.

Implicit in the assumption of a fixed PV gradient is the assumption that the atmosphere is in thermodynamic equilibrium; that is, the time rate of change of temperature is negligible compared to advection of sensible and latent heat by the motions that maintain the constant PV gradient and compared to diabatic heating and cooling. We now add the assumption that energy and moisture transport across isentropes occurs only by deep convection. Thus radiative cooling in the region bounded by two isentropes can only be balanced by turbulent heating from the region of the earth's surface also bounded by those isentropes, or by latent heating due to moisture evaporated from that region, or by deep convection that carries heat and water vapor directly from the surface to some point between those isentropes.

The assumption that energy and moisture cannot be transported across isentropes in the absence of convection can be motivated as follows. Entropy conservation requires that for an atmosphere in thermodynamic equilibrium the net entropy flux across each isentrope be zero. If all latent heat release between two neighboring isentropes is assumed to be derived from water vapor that evaporated in the region at the surface bounded by those isentropes, then since the entropy flux into the region between the two isentropes necessary to balance the difference between net radiative cooling and net latent heat release cannot derive from a net flux across isentropes, it must come from that same surface region, as illustrated in Fig. 7. The assumption that latent heat release takes place on the same isentrope along which it evaporated is supported by the work of Yang and Pierrehumbert (1994), who found that water vapor concentrations in the extratropics can be modeled well by assuming chaotic mixing of water vapor along isentropes. For a discussion of the connection between surface heat fluxes and interior PV fluxes, see Held and Schneider (1999).

These assumptions can be expressed mathematically as

$$F_i = \frac{1}{A_{\theta_a}^{\theta_b}} \int_{\phi_a}^{\pi/2} \int_{p_{\theta_a}}^{p_{\theta_b}} \left[(1 - \alpha)\frac{Q_r}{g}\right] dp 2\pi a^2 \cos\phi \, d\phi + F_c, \quad (8)$$

where F_i is the sum of the sensible (F_{SH}) and latent (F_{LH}) turbulent heat fluxes from the surface to the atmosphere, averaged over the region at the surface between latitudes ϕ_a and ϕ_b; Q_r is the radiative heating rate at a given pressure (p) and latitude (ϕ); a is the earth's radius; θ_a and θ_b are the bounding isentropes; ϕ_a is the latitude where θ_a intersects the earth's surface; α is the fraction of Q_r balanced by convective fluxes (and is discussed in detail below); and $A_{\theta_a}^{\theta_b}$ is the area of the earth's surface bounded by the surface's intersections with θ_a and θ_b. Here, F_c is the flux of heat needed to balance radiative cooling on isentropes that do not intersect the surface outside the Tropics [we will refer to these as ''middle-world'' isentropes, while those that do intersect the surface will be referred to as ''underworld'' isentropes after Hoskins (1991)] plus the fraction α of radiative heating on other isentropes that is balanced by convective rather than large-scale heat fluxes from the surface. Its calculation is discussed in the next section.

We next consider fluxes into the surface mixed layer due to ocean heat transport. An ocean heat flux of 2 PW is consistent with recent estimates of ocean heat transport (Trenberth and Solomon 1994). The accompanying flux convergence is expressed as F_O in Eq. (1) and has the prescribed distribution:

$$F_O = \begin{cases} T_0\omega[-\cos(3.857\phi) - 0.102] \\ \quad \text{for } |\phi| \le 70^\circ \text{ latitude} \\ 0 \quad \text{for } |\phi| > 70^\circ \text{ latitude,} \end{cases} \quad (9)$$

where T_0 is the maximum poleward heat flux (which in this scheme is forced to occur at 23° latitude and equals 2 PW), ω is a geometric factor equal to 9.7924×10^{-15} m^{-2}, and ϕ is latitude in radians. The cutoff at 70° latitude accounts for the Antarctic continent, which prevents any oceanic heat flux south of that latitude in the Southern Hemisphere, and accounts for the negligible annual mean heat flux observed north of that latitude in the Northern Hemisphere (Aagaard and Greisman 1975). The global area weighted mean of F_0 is zero, of course.

f. Convection parameterization

Moist convection occurs when both conditional instability and sufficient dynamic forcing exist so that parcels of air in the boundary layer can be lifted to their level of free convection, at which level their density is lower than that of the surrounding air. It persists when sufficient convergence of heat and moisture exist to maintain conditional instability against the convective redistribution of heat. We will assume that sufficient heat and moisture convergence exist and determine the probability of convection on the basis of the degree of conditional stability alone. We use the *degree* of conditional stability because we expect that, although the zonal and monthly mean vertical temperature profile for a given latitude may be conditionally stable, there will nevertheless be particular locations and times at that latitude where vertical profiles are conditionally unstable, so that the zonal mean convective energy flux will not be zero. These episodes of conditional instability will occur when fluctuations in surface temperature and temperature aloft lead to warmer than average surface temperature and cooler than average temperatures aloft. Thus, the probability that moist convection will occur should depend on the variability of the local surface temperature as well as on the degree of conditional stability of the mean state.

Our convection parameterization works as follows. The proportion of radiative cooling balanced by convection, α, is determined for each grid point in the atmosphere, using the following formula:

$$\alpha = \begin{cases} 1 & \text{for } \theta_m \ge \theta \\ \exp\left(-\dfrac{(\theta_m - \theta)^2}{\hat{\theta}_m}\right) & \text{for } \theta_m < \theta, \end{cases} \quad (10)$$

where

$$\hat{\theta}_m = c\left|\frac{\partial\theta_m}{\partial y}\right|, \quad (11)$$

and where θ is the potential temperature at a given latitude and pressure, θ_m is the potential temperature at that latitude and pressure of a moist adiabat originating at the surface at the same latitude, $\hat{\theta}_m$ is a measure of the variability of θ_m, and c is a tunable parameter that relates local temperature variability to the local temperature gradient. Here, c has units of meters, and so represents a radius over which the mean temperature gradient is mixed to produce local temperature variability. Thus, the product $c|\partial\theta_m/\partial y|$ represents the variability of the temperature at a given latitude. If $c = 0$ m, local temperature variance is zero and convection only occurs when conditional instability exists (i.e., when $\theta \le \theta_m$). If $c > 0$, sufficient temperature variance exists so that convection can sometimes take place, even when $\theta > \theta_m$.

Once α has been calculated everywhere, the net downward convective energy flux through the earth's surface F_c can be determined at each latitude:

$$F_c = \int_{p_s}^{0} \frac{\alpha Q_r}{g} \, dp. \quad (12)$$

Next, α is scaled so that the integral of F_c over the earth's surface is equal to the integral of Q_r in middle-world plus the integral of αQ_r in underworld. We then substitute $(1 - \alpha)Q_r$ for Q_r in Eq. (8), so that the fraction

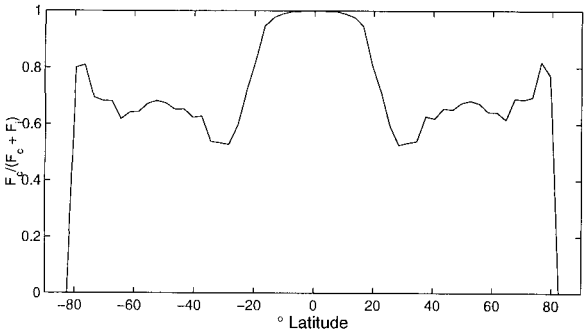

FIG. 8. The ratio $F_c/(F_c + F_i)$ plotted vs latitude.

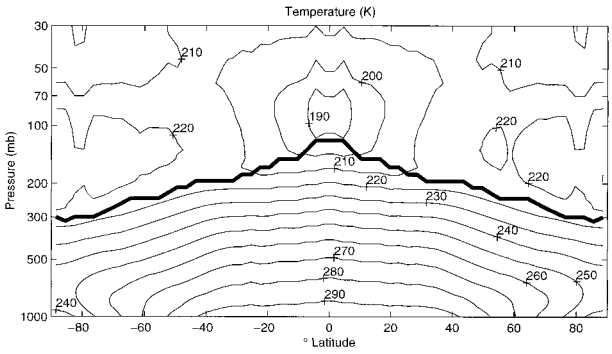

FIG. 9. Model equilibrium temperature as a function of p and ϕ. Contour interval is 8 K. The solid line is the model tropopause.

of radiative cooling *not* accounted for by convection is left to be balanced by surface fluxes along the isentrope on which the radiative cooling occurs.

Figure 8 shows the ratio of F_c, the turbulent surface energy flux that balances convective heating aloft, to $F_c + F_i$, the total turbulent surface energy flux, for $c = 3200$ km. It demonstrates that surface fluxes balancing αQ_r dominate surface fluxes everywhere but are relatively small in midlatitudes. The total surface flux near the Poles is very small, leading to the jumpy ratio there. The dominance of surface fluxes balancing moist convection over surface fluxes balancing isentropic energy budgets does *not* indicate that eddy motions on isentropes are insignificant carriers of energy fluxes. Rather, this dominance reflects the relatively small surface area of the regions, poleward of 45° latitude, where little convection takes place. In addition, since net radiative cooling of isentropes that do not intersect the surface is partially balanced by convection, some of the fluxes contributing to $F_c(\phi)$ are, in fact, balancing radiative cooling in regions poleward of ϕ.

g. Procedure for obtaining an equilibrium climate

Equation (1) can be integrated as follows. The earth's surface is represented by an ocean mixed layer of fixed heat capacity, discretized into an array with 3° latitude resolution (60 points, from −88.5° to 88.5°). It is initialized with an arbitrary initial temperature distribution, and the lapse rate $\partial\theta/\partial p$ is set equal to its (meridionally varying) climatological zonal mean value outside the Tropics. The locations of the boundaries between the Tropics and extratropics in each hemisphere are chosen arbitrarily.

The fluxes $F_{\rm IR}$, $F_{\rm SO}$, $F_{\rm SH}$, and $F_{\rm LH}$ are derived from the surface temperature distribution as follows. The atmosphere is discretized into a pressure–latitude grid, with 3° latitude resolution (60 points, from −88.5° to 88.5°) and 15-mb pressure resolution (68 points, from 8 to 1013 mb). Temperatures in the tropical troposphere are set to moist adiabats originating at the surface. This provides the boundary conditions for the calculation of the extratropical troposphere's temperature. The water vapor mixing ratio is then calculated using prescribed relative humidities. Using the radiative transfer code, we calculate the stratosphere's radiative equilibrium temperature for an initial guess of the tropopause height. The tropopause height is then found using the procedure described above. The static stability is then adjusted so that the potential temperature at each polar tropopause is equal to the potential temperature at the surface at the edge of the Tropics, and the radiative transfer code is run again with the new temperature distribution.

Once the extent and temperature of the stratosphere are known, the temperature and radiative flux and heating rate are known at each point in the atmosphere. The radiative fluxes predicted at the surface can now be applied directly to the surface mixed layer via Eq. (1). Next the surface turbulent heat fluxes must be calculated. To calculate F_i, the integral in Eq. (8) is approximated by summing $(Q_r/g)\delta p 2\pi a^2 \cos\phi\delta\phi$ over all those grid points whose potential temperature is closest to, but not greater than, the potential temperature of each point along the surface. Then F_c is calculated from Eq. (12). The total turbulent heat flux, $F_{\rm SH} + F_{\rm LH}$, is equal to the sum of F_i and F_c.

Next, the radiative, turbulent, and oceanic heat fluxes can be applied to Eq. (1), and the surface temperature adjusted. In the Tropics, the temperature is adjusted to its mean value. Then the new surface temperature distribution is used to generate a new set of fluxes. This process is repeated until equilibrium is approached, that is, when the sum of the fluxes on the rhs of Eq. (1) falls below 0.1 W m^{-2}. In some cases oscillations in the turbulent fluxes require that fluxes be averaged over several time steps to achieve this criterion. The model can also be run with fixed surface temperatures, in which case the overall surface energy flux budget will not, in general, be balanced.

3. Results and sensitivity experiments

Figure 9 shows the equilibrium climate for the model described above, with $\gamma = 1$. Fig. 10 and Figs. 11a and 11b show equilibrium surface temperatures and surface and top-of-the-atmosphere energy fluxes. Model polar

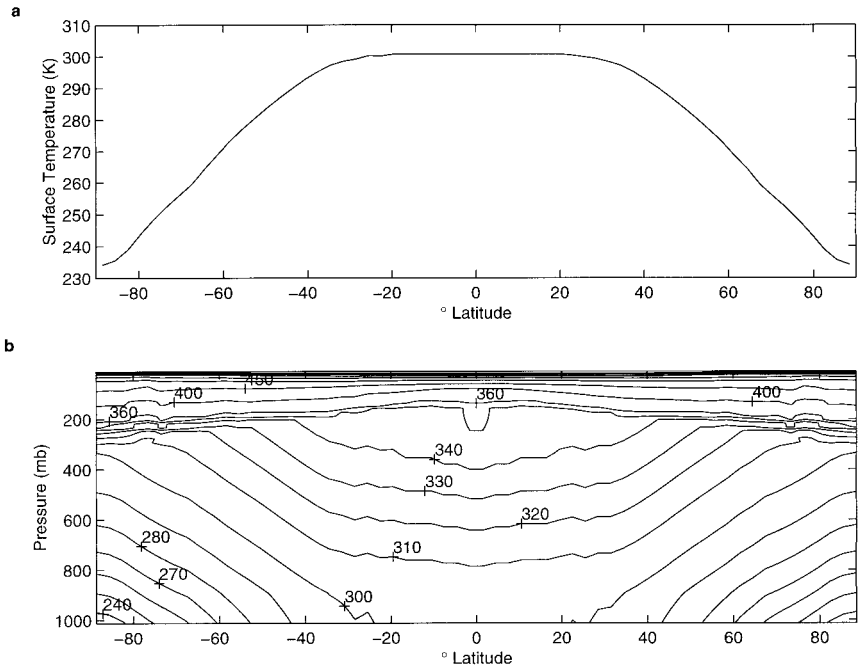

FIG. 10. (a) Equilibrium surface temperatures for control run. (b) Equilibrium potential temperatures aloft.

surface temperatures are significantly cooler than observed temperatures, for reasons we discuss below in the section on surface static stability. We next present results from sensitivity studies involving various model parameters: the surface lapse rate, the imposed PV gradient, the concentration of carbon dioxide, the convection parameter *c*, and the rate of stratospheric overturning.

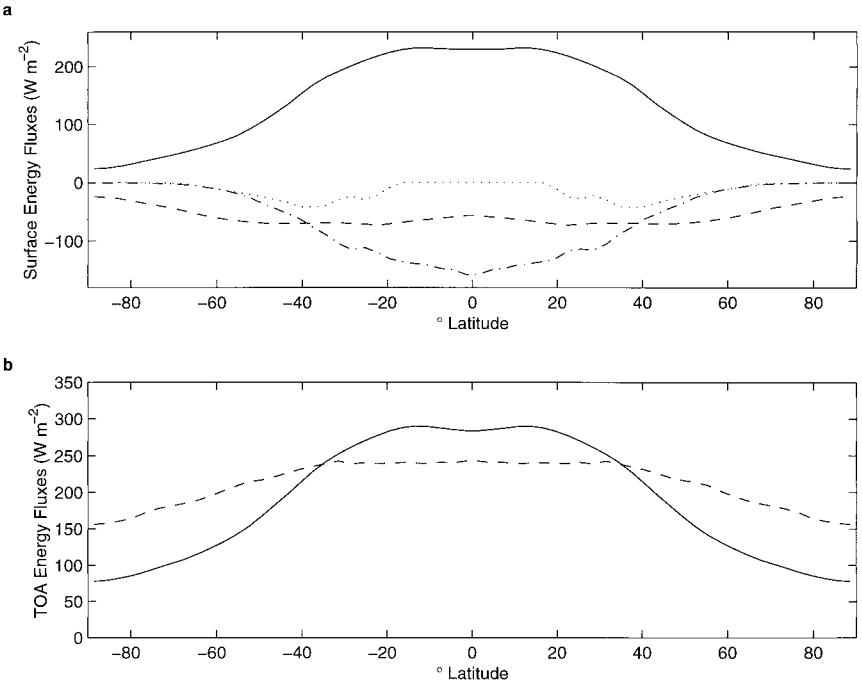

FIG. 11. (a) Equilibrium surface fluxes (solar, solid; infrared, dashed; nonconvective turbulent, dotted; convective, dot-dashed). (b) Equilibrium top-of-atmosphere energy fluxes (downwelling solar, solid; upwelling IR, dashed).

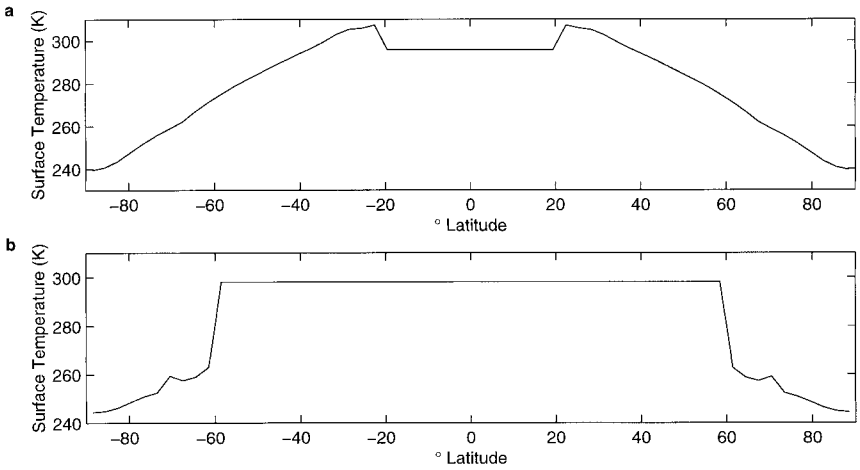

FIG. 12. Model results with no convection scheme. (a) Surface temperature after 3 time steps of model integration, and the edge of the Tropics fixed at 20° latitude. (b) Equilibrium surface temperature, with the edge of the Tropics set to 60° latitude.

a. Convection parameterization

We begin by considering the role of the convective parameterization in setting the climate of the model midlatitudes. This is most dramatically done by completely removing the convection scheme. In this case, we obtain the results shown in Fig. 12. If the edges of the Tropics are held at 20° latitude, the model fails to converge. The surface temperature after 3 time steps is shown in Fig. 12a: temperatures in the Tropics are cooler than temperatures in the subtropics, and the peak temperatures just outside the Tropics are increasing rapidly with time. Integration ceases when temperatures exceed the range for which the radiative code is valid. Figure 12b shows that if the edges of the Tropics are moved poleward to 60° latitude, the model can come to equilibrium, but with a climate that does not much resemble that of the earth: surface temperatures are flat to 60° (which in any case could not be achieved by any circulation with the physics of the real-world Hadley cell) and fall off sharply beyond that point.

This situation arises because the regions outside, but adjacent to, the Tropics have no strong negative feedback on their temperature. As the surface temperature rises, temperatures in the boundary layer and, to a lesser degree, in the free troposphere increase. This leads to increased downwelling radiation, which balances the increase in upwelling radiation due to the surface's warmer temperature. The atmosphere's increased radiative cooling is balanced by fluxes of heat from the Tropics, because most of the atmosphere above points adjacent to the Tropics lies in middle-world. Thus surface temperatures fall in the Tropics and rise in the nearby extratropics, without apparent limit. Only when the edge of the Tropics is moved poleward to the region where solar radiation falls off sharply with latitude do the regions just outside of the model Tropics become cooler than the Tropics.

These results show that for our model, significant cross-isentropic fluxes between the surface and the interior of the free troposphere are necessary for temperatures to fall from the Tropics to the extratropics. This result does not depend on the nature of our assumptions about PV homogenization or about surface static stability, and we believe that it should apply to the real earth as well, with the understanding that ''convection'' in the sense of this model includes the ''slantwise convection'' of midlatitude frontal cyclones as well as deep vertical deep convection.

Figure 13 shows the equilibrium temperature structure for three values of c. When $c = 0$ m, we see that the equilibrium temperature is nearly flat for all latitudes equatorward of 50° latitude. This is because, for this value of c, convection is an all-or-nothing phenomenon. The lapse rate outside the model Tropics is tied to the lapse rate in the Tropics by PV homogenization: when $\gamma = 1$ everywhere in Eq. (6), $\partial\theta/\partial p$ must be constant along θ surfaces. If temperatures outside the Tropics are cooler than temperatures within the Tropics, then if the temperature profile in the Tropics is of marginal conditional stability, the cooler extratropical temperature profile will be conditionally stable, although it has the same lapse rate (Emanuel 1994). Because the temperature of these regions would, in the absence of convection, tend to rise indefinitely (see Fig. 12a), they warm until they reach a surface temperature that makes the vertical temperature profile marginally conditionally unstable. Convection then switches on and then temperature equilibrates.

As c increases, the extratropical temperatures decrease, since it is increasingly likely that convection will occur, even if the zonal mean lapse rate is conditionally stable. Figure 13 shows equilibrium surface temperatures for c equal to 3200 and 4800 km. For the runs to be discussed below, we choose the minimum c (3200

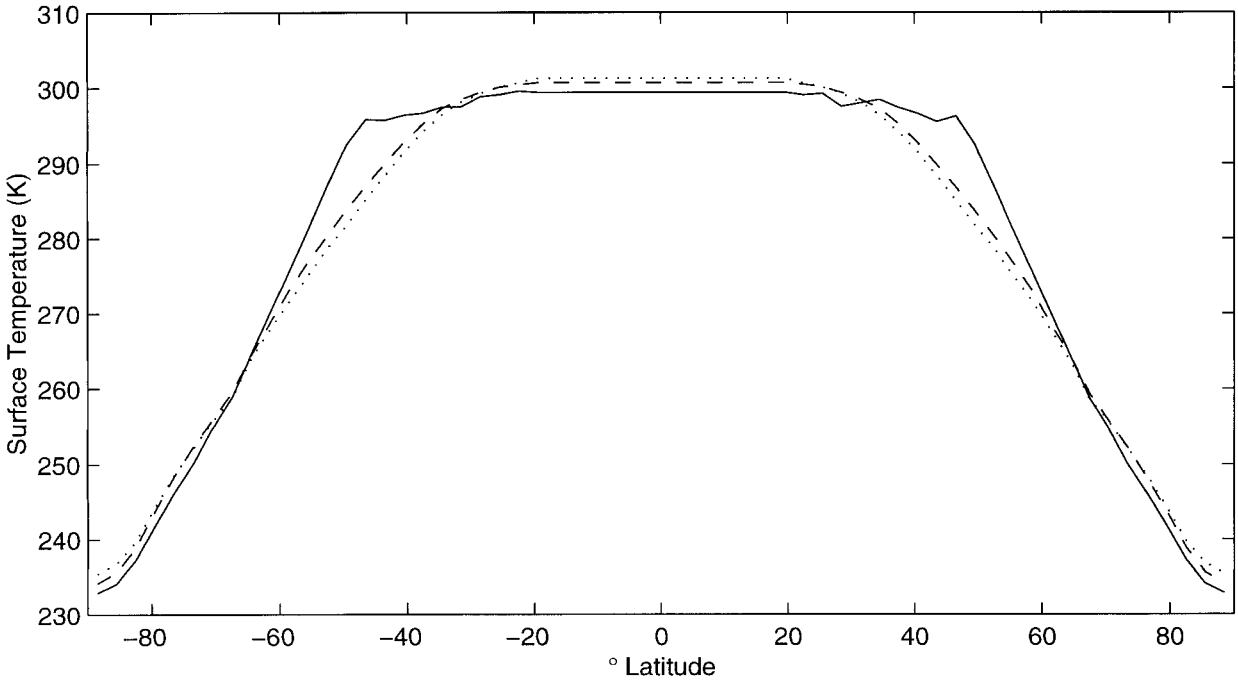

FIG. 13. Equilibrium temperature plotted against latitude for three values of the parameter c: $c = 0$ km (solid), $c = 3200$ km (dashed), $c = 4800$ km (dotted).

km) so that temperature decreases monotonically from the equator to the Poles. This value is of the order of the Rossby radius.

b. The height of the tropopause and stratospheric overturning

Figure 9 shows that while the temperature structure in the vicinity of the tropopause is similar to observations, the model tropopause itself is still too low in the Tropics (120 mb, vs 90 mb in observations). The location of the coldest temperature, however, is now in good agreement with observations. This discrepancy can be attributed to the fact that in the model, the region of coldest temperatures is located in the stratosphere, and lapse rates there are determined solely by radiation and the imposed overturning. In the real tropical upper troposphere, there is a more gentle transition between the region where lapse rate is strongly influenced by convection and the region where radiative forcing takes over (Thuburn and Craig 1997).

As shown in Fig. 14, comparison of model runs with different imposed PV gradients shows that the height of the tropopause is fairly insensitive to substantial changes in the tropospheric temperature structure. Polar tropopause temperature falls by about 5 K, and tropopause height descends by about 40 mb as the PV gradient decreases from $\gamma = 2.0$ to $\gamma = 0.0$ in these model runs made with fixed surface temperature and fixed surface static stability. Similar experiments were run with γ held fixed, and with surface static stability fixed at various values, and a small range in polar tropopause temperature and height for a large range in surface static stabilities was found. These results are consistent with those of Held (1982), who found little sensitivity of tropopause height to tropospheric lapse rate. This led us to consider whether changes in the strength of the stratospheric overturning circulation would have much impact on the model tropopause height and temperature.

When the overturning rate was adjusted, the results were dramatic. As shown in Fig. 15, the tropopause height predicted for zero overturning circulation has very little latitude dependence, nor do large variations in the imposed PV gradient result in substantial change in tropopause height and/or temperature. Compared to observations shown in Fig. 16, the model tropopause is 10 K too warm in the Tropics and about 100 mb too low, while in the polar regions it is some 10 K too cold and 150 mb too high.

Figure 17 confirms that when γ and surface static stability are held fixed, variations in stratospheric overturning rate, expressed as the maximum tropical stratospheric radiative cooling rate, lead to dramatic changes in tropopause height. Thus for a model stratosphere where air rises in the polar regions and falls near the equator, the shape of the tropopause is exactly the opposite of the observed shape, high in the Poles and low near the equator. These results show that in the model climate, the stratospheric overturning circulation alone determines the meridional shape of the tropopause. They

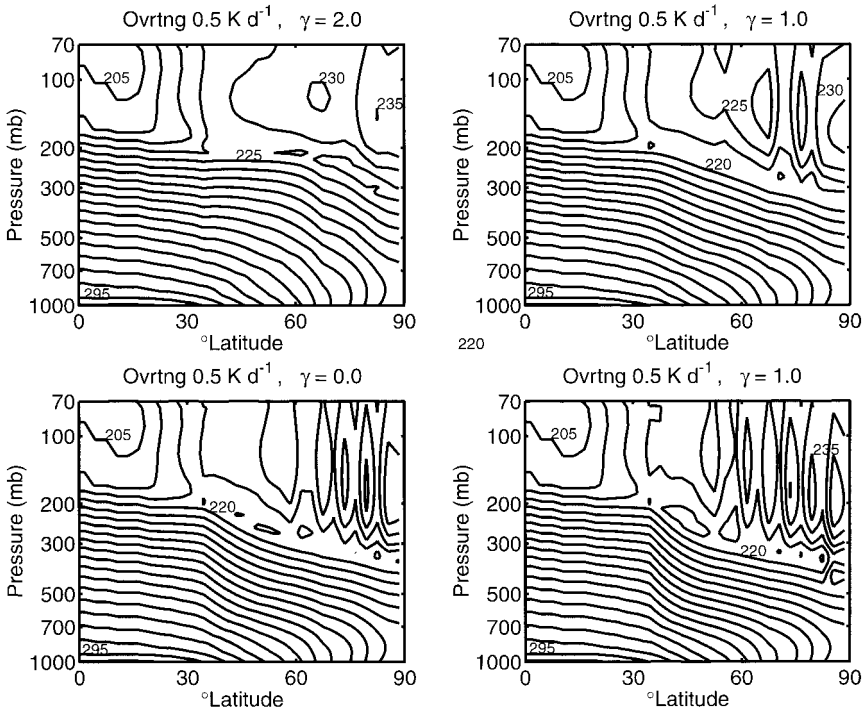

FIG. 14. Contours of temperature plotted vs p and ϕ, for various values of γ, with standard overturning circulation. Contour interval 5 K.

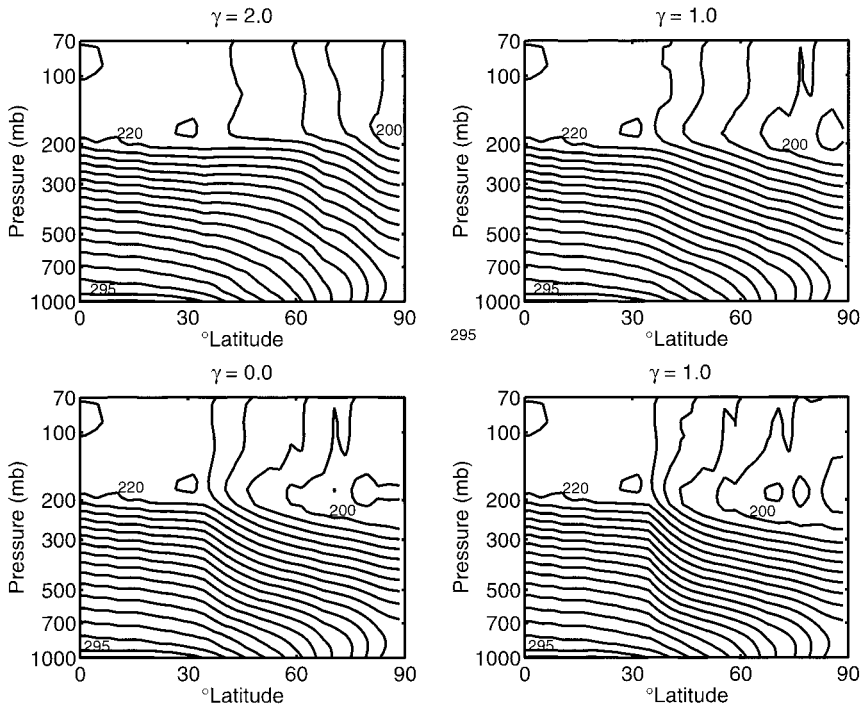

FIG. 15. Contours of temperature plotted vs p and ϕ, for various values of γ and no overturning circulation. Contour interval 5 K.

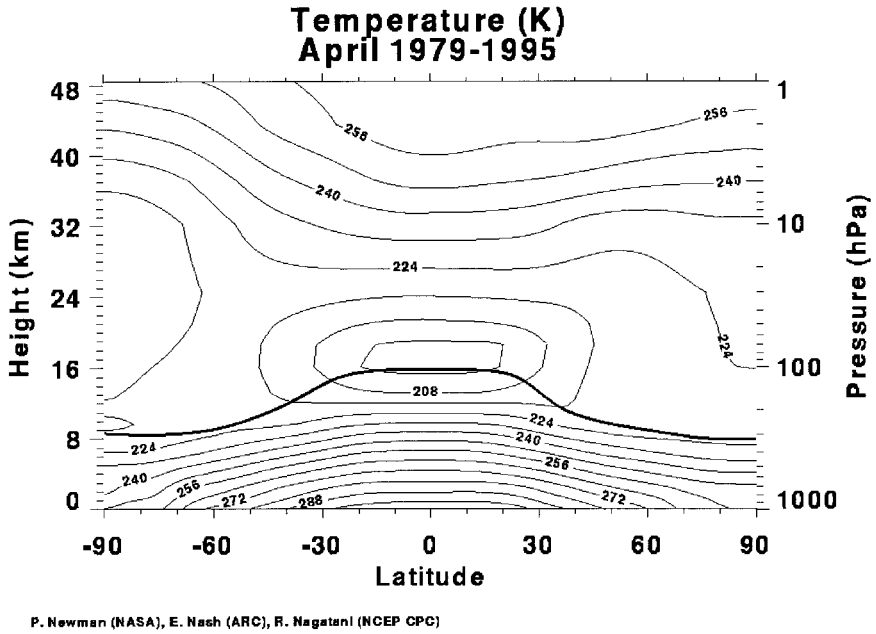

FIG. 16. Observed zonal mean Apr temperature as a function of p and ϕ. The bold line is the tropopause, as defined by the WMO: the lowest level at which the lapse rate decreases to 2 K km^{-1}, provided that the average lapse rate between this level and all higher levels within 2 km does not exceed 2 K km^{-1}. Data from NCEP–NCAR reanalysis (courtesy of P. Newman).

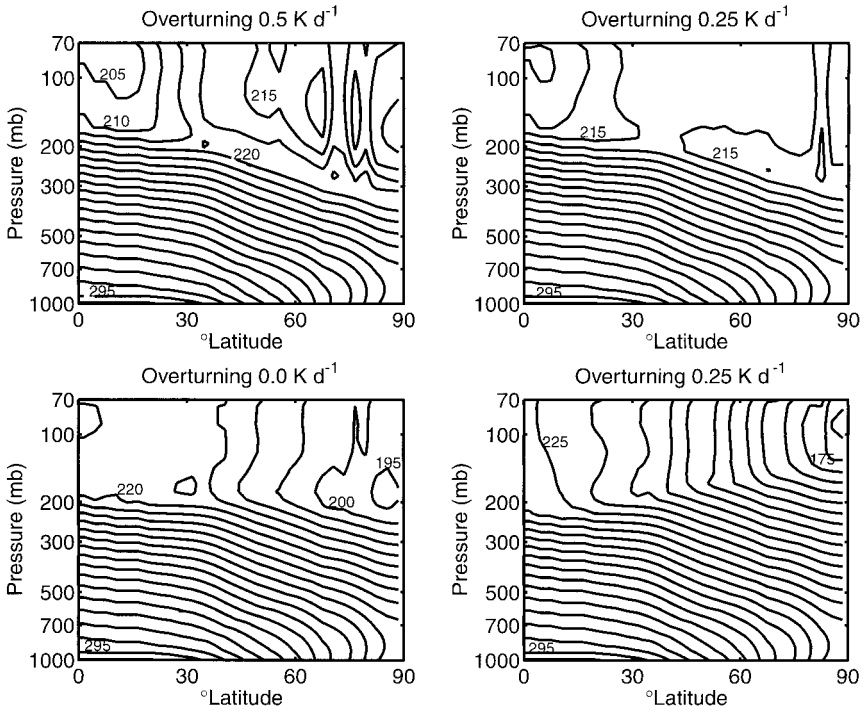

FIG. 17. Temperature contours plotted vs p and ϕ, for various values of overturning circulation strength, expressed as the maximum stratospheric radiative cooling rate. Contour interval 5 K.

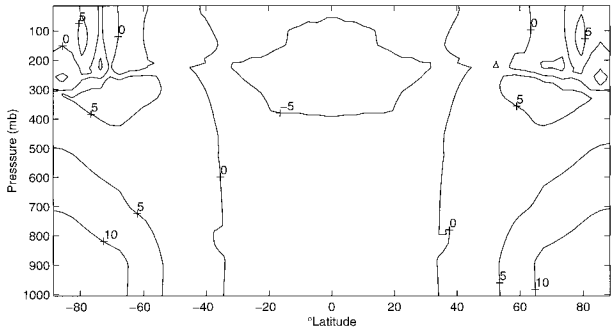

FIG. 18. Change in equilibrium temperature when the surface static stability is increased by 5% and held fixed.

suggest that the same may be the case in the real atmosphere.

c. Surface lapse rate

Figure 18 shows the model's sensitivity to a 5% increase in the surface lapse rate, $\partial\theta/\partial p$, with the static stability held fixed, and the polar tropopause θ allowed to differ from the equatorial surface θ. Equilibrium surface temperatures increase by up to 8 K in polar regions, while decreasing by about 0.5 K in the Tropics. This pattern of temperature change can be understood as follows: an increase in static stability in the polar regions leads to warmer temperatures aloft relative to surface temperatures. This implies a larger net downwelling of infrared radiation, as well as larger radiative cooling rates aloft, as shown in Fig. 19. The increase in net downwelling radiation at a given latitude tends to heat the surface locally, but the enhanced radiative cooling is always balanced by surface fluxes distributed equatorward of that latitude. This means that the polar regions are able to warm at the expense of the Tropics, and this implies an increase in meridional energy transport, consistent with the reduced equilibrium temperature gradient. Similar experiments (not shown) show that increasing cloud fraction leads to a decrease in the equator-to-Pole temperature difference, as a more emissive atmosphere increases the implied meridional energy transport at equilibrium.

d. PV gradient

Figure 20a shows results from experiments in which the magnitude of the imposed PV gradient was varied. In the real atmosphere, we would expect more vigorous mixing of PV to be accompanied by more vigorous meridional energy fluxes and thus a weakened temperature gradient. Decreasing PV gradient from $\gamma = 1.0$ to $\gamma = 0.6$ results in a decreased surface temperature gradient. In the next section it will be shown that this connection implies a negative feedback to global radiative perturbations and a strong negative feedback to polar sensitivity.

Experiments were also run in which the magnitude of the imposed PV gradient was varied, while surface static stability was held fixed. Thus, our condition on the polar tropopause could no longer be maintained. Figure 20b shows that as the PV gradient decreases from $\gamma = 1.0$ to $\gamma = 0.6$, the meridional temperature gradient tends to increase. This result is somewhat counterintuitive: in the real atmosphere, we would expect motions that mix potential vorticity more effectively in order to mix heat more effectively as well. Analysis of the 2D structure of temperature change shows that the cause of this behavior is as follows. A stronger PV gradient implies higher values of PV itself in the polar regions and thus larger static stability there. If temperature is integrated from the bottom up (as fixed surface static stability implies), the higher polar PV must mean a stronger polar inversion, which gives warmer temperatures aloft, relative to the surface. As explained in the previous

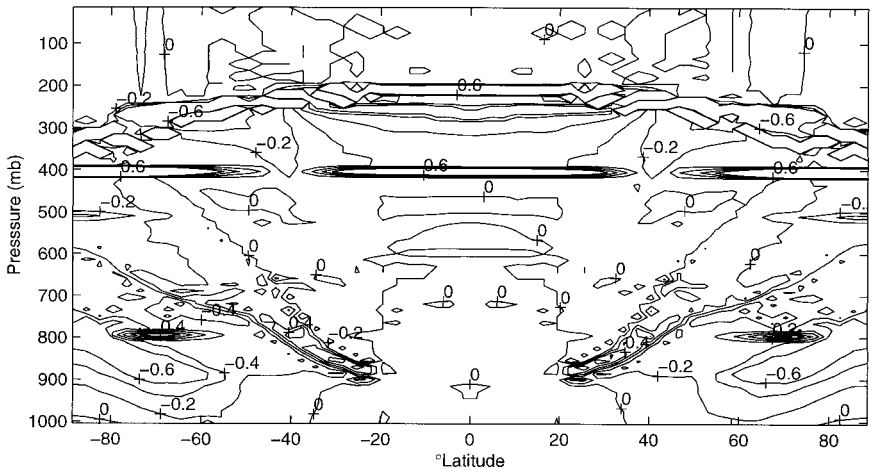

FIG. 19. Change in equilibrium radiative heating rate when the surface static stability is increased by 5% and held fixed.

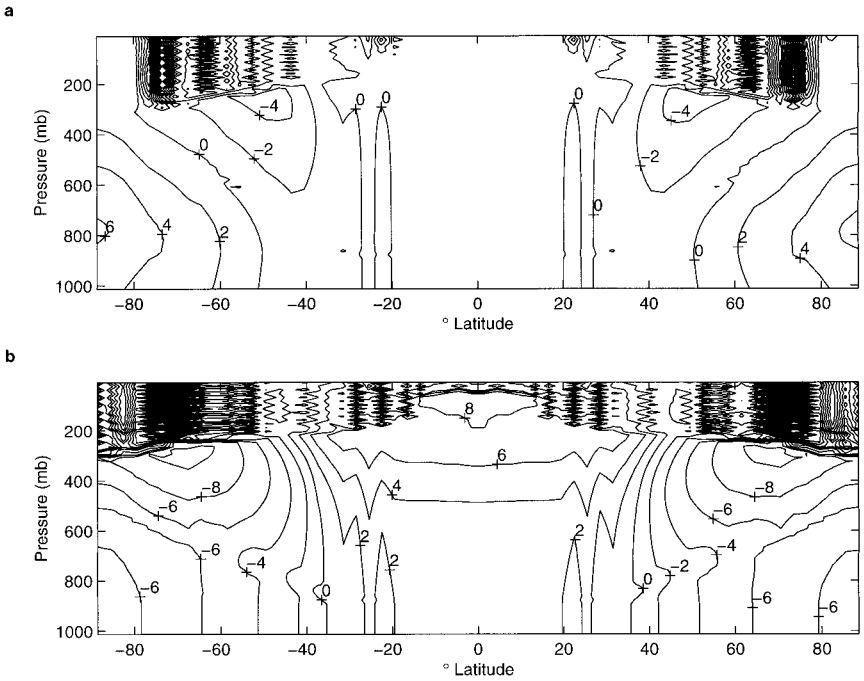

FIG. 20. Change in equilibrium temperature when the tropospheric PV gradient is decreased from $\gamma = 1.0$ to $\gamma = 0.6$ for (a) surface static stability adjusted so that the isentrope leaving the boundary layer at the edge of the Tropics intersects the tropopause at each Pole and (b) constant surface static stability.

section, the effect of this is to warm the polar surface at the expense of the midlatitude and tropical surface. This accounts for similar behavior found in Sun and Lindzen (1994).

e. Carbon dioxide

Figure 21b shows the change in temperature when the model CO_2 is doubled from 300 to 600 ppmv and surface static stability is held fixed, as is the relative humidity by assumption. This, therefore, is not meant to be an evaluation of climate sensitivity per se. Rather, we wish to examine the implications of the present model for the structure of the response. Note the poleward amplification of temperature increase. This occurs because an initial warming at the Poles leads to warmer temperatures aloft (due to the fixed surface static stability and fixed PV gradient), which result in increased downwelling infrared fluxes from the atmosphere to the surface. These fluxes further warm the polar surface, while the associated radiative cooling of the atmosphere must be balanced by surface heat fluxes from regions closer to the equator.

The meridional pattern of sensitivity to CO_2 is different when the static stability is adjusted to make the isentrope leaving the boundary layer at the edge of the Tropics intersect the tropopause at the Poles (Fig. 21a). In this case, there is a strong poleward *diminution* of the surface temperature change. Warming is about 1 K in the Tropics, increases to about 2 K in midlatitudes, and falls nearly to zero at the Poles. The overall global sensitivity falls from 1.5 K to 1.2 K. The cause of this change in sensitivity is as follows. With fixed surface static stability, temperatures near the polar tropopause tend to warm more than temperatures near the tropical surface. If the polar tropopause is required to lie along an adiabat originating at the tropical surface, its temperature change is forced to be smaller than the temperature change at the tropical surface. Since temperatures at the polar tropopause depend on surface temperatures everywhere, and since the surface temperature change in midlatitudes is larger than the change in the Tropics for the reasons outlined in the previous paragraph, polar surface static stability must be reduced to maintain temperature continuity between the polar surface and polar tropopause. This reduction in static stability means that temperatures aloft in the polar regions become cooler relative to the surface, which reduces the downwelling infrared radiation at the surface, thus resisting the initial warming due to increased carbon dioxide concentration.

4. Discussion and conclusions

The construction of the energy balance climate model described above and its integration to equilibrium demonstrate that an assumption of PV homogenization together with additional assumptions about the temperature structure of the Tropics and the static stability of the planetary boundary layer, are sufficient to constrain

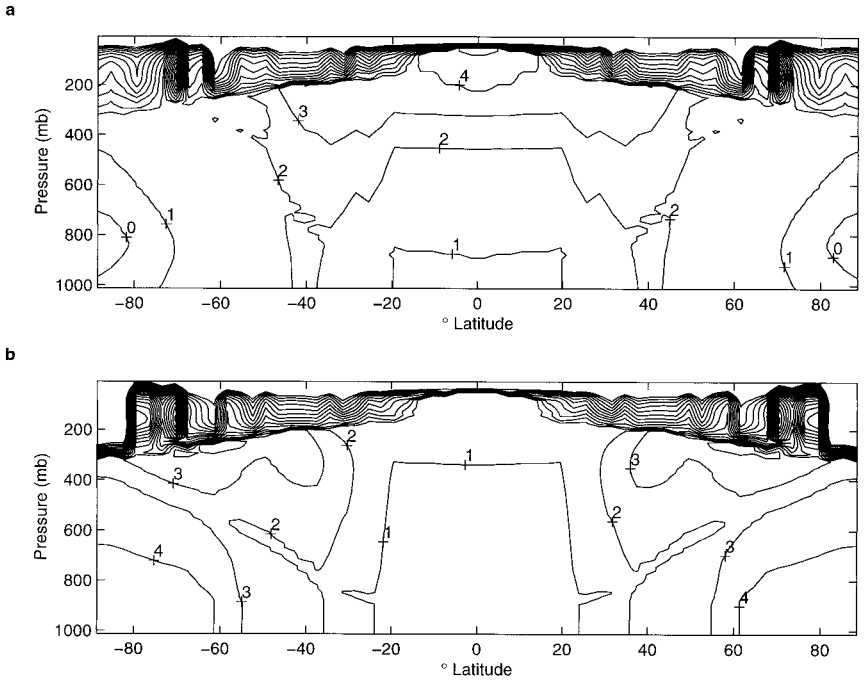

FIG. 21. Change in equilibrium temperature when the concentration of CO_2 is increased from 300 to 600 ppmv for (a) surface static stability adjusted so that the isentrope leaving the boundary layer at the edge of the Tropics intersects the tropopause at each Pole and (b) constant surface static stability.

the earth's zonal mean climate. This helps to establish the feasibility of a baroclinic neutralization mechanism such as that envisioned by Lindzen (1993), where eddies act to mix PV, thus stabilizing the mean flow to the eddies' further growth, and simultaneously to establish the earth's zonal mean temperature structure. However, our results also reveal the incompleteness of this mechanism as a theory of the zonal mean climate. We show that an imposed PV gradient alone does not strongly constrain the meridional temperature gradient, since the determination of the surface static stability is at least as important to the specification of the PV in determining model climate.

Our assumption that the isentrope leaving the Tropics intersect the polar tropopause is essentially a way to apply an integral constraint on the surface PV distribution. It is based on observations that suggest this assumption works well through seasonal variations of the earth's zonal mean temperature structure, but it is presently without theoretical justification. It is to be hoped that further work may obviate the need for such an arbitrary closure.

Sensitivity tests using our model indicate that the meridional slope of the tropopause is due not to any tropospheric factor, but rather to the overturning of the stratosphere, and the resulting warming and cooling terms introduced in the polar and equatorial regions, respectively. While the importance of the overturning circulation in setting the temperature of the tropopause is well known (Holton et al. 1995), we are not aware of previous discussion of the influence of the Brewer–Dobson (Brewer 1949; Dobson 1956) circulation on the meridional distribution of tropopause height. Left unexplained by our model is the sharpness of the jump in tropopause height at the subtropical jet. This is likely to be a consequence of our neglect of momentum conservation in the Hadley cell. In the real atmosphere, this tends to ensure a sharp temperature gradient at the edge of the Tropics, in balance with the subtropical jet, while the model atmosphere has a smoothly falling temperature structure at the edge of the Tropics.

The necessity of allowing some cross-isentropic transport in order to properly simulate the transition between the Tropics and extratropics shows clearly the importance of deep convection in determining the climate of the extratropical regions. In addition, the inductive approach used here demonstrates one of the advantages of simple models in understanding the mechanisms that establish the earth's climate. By contrast, it would be difficult to ''shut off'' cross-isentropic transport in a GCM. Elimination of the convection parameterization would only result in the model representing moist convection explicitly.

The dependence of the meridional response of the model climate to an increase in carbon dioxide on the specification of surface static stability demonstrates the importance of the lapse rate feedback. Delicate adjustments to the relationship between surface temperatures

and temperatures aloft were shown to have a strong impact on the meridional profile of model climate change. The strong sensitivity of the polar climate to the specification of surface static stability also raises some interesting questions about the maintenance of the polar climate, especially its ''coreless winter,'' during which temperatures vary little over two to three months. In future work we will address these questions and connect them to the discussion of links between PV homogenization and surface static stability introduced here.

Acknowledgments. The authors thank F. Drake for making available his zonal mean analysis of ISCCP data. The suggestions of two anonymous reviewers helped us to improve this article's flow and to reduce its grandiosity.

A large portion of the work on this article was done as part of DBK's Ph.D. thesis at MIT under the supervision of RSL. DBK thanks RSL for patience and inspiration. The article was completed at Harvard University, where DBK is supported by NASA Grant NAG-1-1849. At MIT, this work was partly supported by an NSF Graduate Fellowship and partly by NSF Grant ATM-9421195, DOE-CHAMMP award DEFG02-93ERG1G73, and NASA Grant NAG5-6304.

REFERENCES

Aagaard, K., and P. Greisman, 1975: Toward new mass and heat budgets for the Arctic Ocean. *J. Geophys. Res.,* **80,** 3821–3827.

Bretherton, F. P., 1966: Critical layer instability in baroclinic flows. *Quart. J. Roy. Meteor. Soc.,* **92,** 325–334.

Brewer, A. M., 1949: Evidence for a world circulation provided by the measurement of helium and water vapor distribution in the stratosphere. *Quart. J. Roy. Meteor. Soc.,* **75,** 351–363.

Brown, R., and C. S. Bretherton, 1997: A test of the strict quasi-equilibrium theory on long time and space scales. *J. Atmos. Sci.,* **54,** 624–638.

Charney, J. G., and M. E. Stern, 1962: On the stability of internal baroclinic jets in a rotating atmosphere. *J. Atmos. Sci.,* **19,** 159–172.

Chou, M.-D., 1986: Atmospheric solar heating rate in the water vapor bands. *J. Climate Appl. Meteor.,* **25,** 1532–1542.

——, and M. J. Suarez, 1994: An efficient thermal radiation parameterization for use in general circulation models. NASA Tech. Memo. 104606, Vol. 3., 85 pp. [Available from NASA Goddard Space Flight Center, Greenbelt, MD 20771.]

Dobson, G. M. B., 1956: Origin and distribution of polyatomic molecules in the atmosphere. *Proc. Roy. Soc. London,* **236A,** 187–193.

Drake, F., 1993: Global cloud cover and cloud water path from *ISCCP C2* data. *Int. J. Climatol.,* **13,** 581–605.

Dütsch, H. U., 1978: Vertical ozone distribution on a global scale. *Pure Appl. Geophys.,* **116,** 511–529.

Eluszkiewicz, J., D. Crisp, R. G. Grainger, A. Lambert, A. E. Roche, J. B. Kumer, and J. L. Mergenthaler, 1997: Sensitivity of the residual circulation diagnosed from the *UARS* data to the uncertainties in the input fields and to the inclusion of aerosols. *J. Atmos. Sci.,* **54,** 1739–1757.

Emanuel, K. A., 1994: *Atmospheric Convection.* Oxford University Press, 580 pp.

——, J. D. Neelin, C. S. Bretherton, 1994: On large-scale circulations in convecting atmospheres. *Quart. J. Roy. Meteor. Soc.,* **120,** 1111–1143.

Goody, R., 1995: *Principles of Atmospheric Physics and Chemistry.* Oxford University Press, 324 pp.

Held, I. M., 1982: On the height of the tropopause and the static stability of the troposphere. *J. Atmos. Sci.,* **39,** 412–417.

——, and T. Schneider, 1999: The surface branch of the zonally averaged mass transport circulation in the troposphere. *J. Atmos. Sci.,* **56,** 1688–1697.

Holton, J. R., P. H. Haynes, M. E. McIntyre, A. R. Douglass, R. B. Rood, and L. Pfister, 1995: Stratosphere–troposphere exchange. *Rev. Geophys.,* **33,** 403–439.

Hoskins, B. J., 1991: Towards a PV-θ view of the general circulation. *Tellus,* **43,** 27–35.

Kalnay, E., and Coauthors, 1996: The NCEP/NCAR 40-year Reanalysis Project. *Bull. Amer. Meteor. Soc.,* **77,** 437–471.

Lindzen, R. S., 1993: Baroclinic neutrality and the tropopause. *J. Atmos. Sci.,* **50,** 1148–1151.

——, and B. Farrell, 1980: The role of the polar regions in global climate, and a new parameterization of global heat transport. *Mon. Wea. Rev.,* **108,** 2064–2079.

Nakamura, N., 1998: Baroclinic–barotropic adjustments in a meridionally wide domain. *J. Atmos. Sci.,* **56,** 2246–2260.

Neftel, A., H. Friedli, E. Moor, H. Lötscher, H. Oeschger, U. Siegenthaler, and B. Stauffer, 1994: Historical CO_2 record from the Siple Station ice core. *Trends '93: A Compendium of Data on Global Change,* T. A. Boden et al., Eds., Oak Ridge National Laboratory, 11–14.

Olaguer, E. P., H. Yang, and K. K. Tung, 1992: A reexamination of the radiative balance of the stratosphere. *J. Atmos. Sci.,* **49,** 1242–1263.

Peixoto, J. P., and A. H. Oort, 1992: *Physics of Climate.* American Institute of Physics, 520 pp.

Rind, D., and M. Chandler, 1991: Increased ocean heat transports and warmer climate. *J. Geophys. Res.,* **96,** 7437–7461.

Sellers, W. D., 1969: A global climatic model based on the energy balance of the earth–atmosphere system. *J. Appl. Meteor.,* **8,** 392–400.

Solomon, A. B., 1998: The role of large-scale eddies in the nonlinear equilibration of a multi-level quasi-geostrophic model. Ph.D. thesis, Massachusetts Institute of Technology, 234 pp. [Available from Document Services, MIT, 160 Memorial Drive, Cambridge, MA 02139.]

Stone, P. H., 1978: Baroclinic adjustment. *J. Atmos. Sci.,* **35,** 561–571.

Sun, D., and R. S. Lindzen, 1994: A PV view of the zonal mean distribution of temperature and wind in the extratropical troposphere. *J. Atmos. Sci.,* **51,** 757–772.

Thuburn, J., and G. C. Craig, 1997: GCM test of theories for the height of the tropopause. *J. Atmos. Sci.,* **54,** 869–882.

Trenberth, K. E., and A. Solomon, 1994: The global heat balance: Heat transports in the atmosphere and ocean. *Climate Dyn.,* **10,** 107–134.

Yang, H., and R. T. Pierrehumbert, 1994: Production of dry air by isentropic mixing. *J. Atmos. Sci.,* **51,** 3437–3454.